

Gapless spin-liquid state in the structurally disorder-free triangular antiferromagnet NaYbO₂

Lei Ding,^{1,*} Pascal Manuel,¹ Sebastian Bachus,² Franziska Grübler,² Philipp Gegenwart,² John Singleton,³ Roger D. Johnson,⁴ Helen C. Walker,¹ Devashibhai T. Adroja,^{1,5} Adrian D. Hillier,¹ and Alexander A. Tsirlin²

¹ISIS Facility, Rutherford Appleton Laboratory, Harwell Oxford, Didcot OX11 0QX, United Kingdom

²Experimental Physics VI, Center for Electronic Correlations and Magnetism, University of Augsburg, 86135 Augsburg, Germany

³National High Magnetic Field Laboratory, Los Alamos National Laboratory, Los Alamos, NM 87545, United States

⁴Clarendon Laboratory, Department of Physics, University of Oxford, Oxford OX1 3PU, United Kingdom

⁵Highly Correlated Matter Research Group, Physics Department, University of Johannesburg, Auckland Park 2006, South Africa

(Dated: November 28, 2021)

We present the structural characterization and low-temperature magnetism of the triangular-lattice delafossite NaYbO₂. Synchrotron x-ray diffraction and neutron scattering exclude both structural disorder and crystal-electric-field randomness, whereas heat-capacity measurements and muon spectroscopy reveal the absence of magnetic order and persistent spin dynamics down to at least 70 mK. Continuous magnetic excitations with the low-energy spectral weight accumulating at the *K*-point of the Brillouin zone indicate the formation of a novel spin-liquid phase in a triangular antiferromagnet. This phase is gapless and shows a non-trivial evolution of the low-temperature specific heat. Our work demonstrates that NaYbO₂ practically gives the most direct experimental access to the spin-liquid physics of triangular antiferromagnets.

Introduction. Quantum spin liquids (QSLs) in frustrated magnets have attracted a lot of attention because of the occurrence of unconventional ground states, where highly entangled spins and their strong fluctuations are observed in the absence of long-range order down to zero temperature. The ensuing excitations are interesting in their own right as they are distinct from magnons in systems with conventional long-range magnetic order [1–3]. Historically, the QSL was first exemplified by the nearest-neighbor resonating-valence-bond (RVB) state on the triangular lattice [4], which drew a great deal of interest in triangular antiferromagnets ever since, although the majority of real-world triangular materials order magnetically at low temperatures [5].

Recently, a promising QSL candidate YbMgGaO₄ with the effective spin-1/2 Yb³⁺ ion on triangular lattice has been proposed by Li *et al.* [6, 7]. They observed persistent spin dynamics down to at least 48 mK [8] and the $T^{0.7}$ power-law behavior of the specific heat [6], indicative of the gapless U(1) QSL characterized by a Fermi surface of fractionalized (spinon) excitations. Although continuous spinon-like excitations were indeed observed experimentally [9], their assignment to spinons [10] is far from unambiguous, and alternative phenomenological explanations within the valence-bond framework were proposed as well [11, 12]. Moreover, absent magnetic contribution to the thermal conductivity [13], considerable broadening of spin-wave excitations in the fully polarized state [14], and acute broadening of the crystal-electric-field (CEF) excitations of Yb³⁺ [15] reveal a significant complexity of this material. The problem appears to be related to the statistical distribution of Mg²⁺ and Ga³⁺ that randomizes the local environment of Yb³⁺ [15] and may lead to peculiar effects like spin-liquid mimicry [16, 17], although the exact influence of the structural randomness (disorder) on the magnetic parameters remains debated [18]. Whether or not these structural effects are integral to the spin-liquid formation, the complexity of YbMgGaO₄ hinders its use as a reference model material for the QSL state in triangular antiferro-

magnets.

On the theory side, significant efforts were made to establish the parameter regime where long-range magnetic order gives way to a QSL. Whereas nearest-neighbor Heisenberg interactions on the triangular lattice support the 120° magnetic order [19], a weak second-neighbor coupling is sufficient to suppress this order and drive the system toward a QSL state [20–27]. The presence of multiple anisotropic interactions—a characteristic of the Yb³⁺ compounds—lays out another route to the QSL [28, 29]. These two regimes, the second-neighbor isotropic exchange vs. nearest-neighbor anisotropic exchange, may in fact produce isomorphic QSL phases [28], but their exact nature and even the presence [22, 26] or absence [20, 23, 24] of a spin gap therein remain vividly debated. Experimental input is thus highly desirable, but requires a disorder-free material characterized down to mK temperatures, as magnetic interactions in the Yb³⁺ oxides are of the order of 1 K, and the ground-state regime is practically reached below 0.4 K only [6, 8].

Na-based chalcogenides NaYbX₂ (X = O, S, Se) have recently come to the attention of researchers as disorder-free triangular antiferromagnets [30, 31]. They feature layers of edge-sharing YbO₆ octahedra with the triangular arrangement of the magnetic Yb³⁺ ions. These layers are separated by the well-ordered Na atoms, with the interlayer Yb–Yb distance of 5.82 Å, which is shorter than in YbMgGaO₄ (8.61 Å), but still significantly longer than the nearest-neighbor Yb–Yb distance of 3.34 Å within the triangular planes (see Fig. 1(a-b)).

Here, we confirm the absence of structural disorder and report persistent spin dynamics in NaYbO₂ down to at least 70 mK. We also observe continuous excitations that are qualitatively similar to those predicted [28] for the QSL state in triangular antiferromagnets. Our results set up NaYbO₂ as a new, disorder-free spin-liquid candidate, and shed light onto the physics of the spin-liquid state in triangular antiferromagnets. We demonstrate gapless nature of this state and the absence of simple power-law scaling for the specific heat.

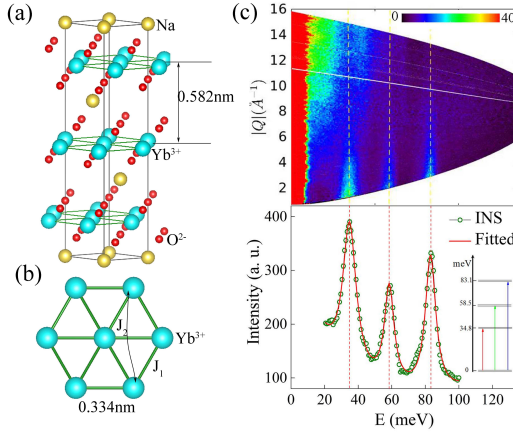


FIG. 1. (a) Stacking of the Yb^{3+} triangular-layers along the c -axis. (b) Triangular layer formed by Yb^{3+} cations. (c) Inelastic neutron scattering spectra $S(Q, \hbar\omega)$ at 5 K with $E_i=150$ meV. Energy dependence of the INS intensity at 5 K integrated in Q over the range 3.9–4.4 \AA^{-1} . Inset depicts the CEF transitions from the ground-state Kramers doublet.

Absence of structural disorder. Polycrystalline samples of NaYbO_2 were synthesized by a solid-state reaction as described in Ref. 32. The absence of structural disorder was verified by synchrotron x-ray and neutron diffraction data [33] collected, respectively, at the ID22 beamline of the ESRF and at the WISH instrument [34] at the ISIS facility. No signatures of site deficiency or disorder was observed in the structure refinements performed down to 1.5 K. The high-resolution synchrotron data reveal very sharp peaks and exclude any extended defects that may occur in a layered compound [33]. At 10 K, the atomic displacement parameter of Yb is below 10^{-3}\AA^2 and excludes any off-center displacements that have been the most direct signature of structural randomness in YbMgGaO_4 [15].

In YbMgGaO_4 , the structural disorder becomes most conspicuous in the CEF excitations that broaden and even show four peaks in the inelastic neutron spectrum [15], instead of the three peaks expected for Yb^{3+} with its $^2F_{7/2}$ multiplet split into four Kramers doublets by the trigonal crystal field [35, 36]. The CEF excitations of NaYbO_2 were measured at 5 K using the MERLIN spectrometer at ISIS operating with the incident energies of 90 and 150 meV [37]. As shown in Fig. 1(c), three sharp, resolution-limited CEF excitations are observed, as expected for Yb^{3+} . This ultimately proves the absence of structural disorder in our material.

From the excitation energies and line intensities we extract the CEF parameters and the compositions of the four Kramers doublets [33]. It is worth noting that the excitation energies of 34.8, 58.5, and 83.1 meV are not far from those reported for YbMgGaO_4 (39.4, 61.3, and 96.6 meV, respectively [15]), reflecting similar local environments of Yb^{3+} in both compounds. By contrast, NaYbS_2 bears all CEF excitations below 50 meV [30], likely in agreement with the less ionic nature of the Yb–S bonds. Similar CEF excitations in YbMgGaO_4 and NaYbO_2 indicate that on the level of single-ion physics the

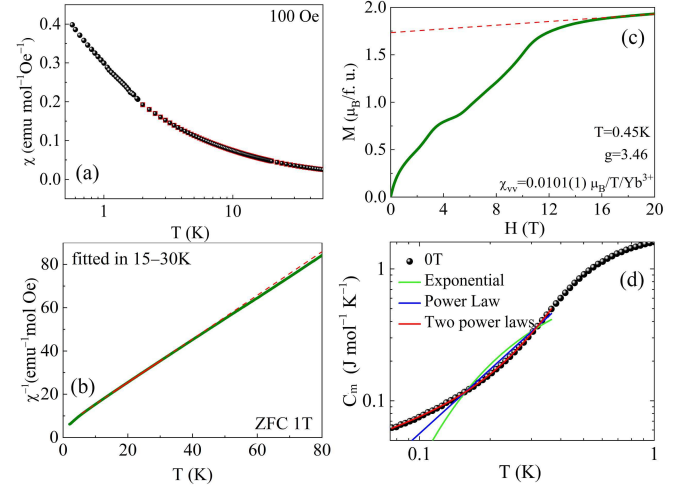


FIG. 2. (a) Temperature dependence of the magnetic susceptibility of NaYbO_2 down to 0.4 K. Zero-field-cooling and field-cooling curves are shown down to 1.8 K. (b) The Curie-Weiss fit to the inverse magnetic susceptibility in the range of 15–30 K after subtracting the Van Vleck term. (c) Isothermal magnetization curve measured at 0.45 K up to 60 T. The red line marks the Van Vleck contribution. (d) Zero-field specific heat of NaYbO_2 with the nuclear contribution subtracted [33].

latter can be seen as a close analogue of the former, but with the structural disorder completely removed.

Ground-state CEF doublet. At low temperatures, the magnetic behavior of NaYbO_2 is fully determined by the ground-state Kramers doublet and can be described by an effective pseudospin- $\frac{1}{2}$ Hamiltonian [38]. Indeed, inverse magnetic susceptibility measured using a SQUID magnetometer (Quantum Design, MPMS-7T) shows a change in slope around 70 K, with the low-temperature linear part reflecting the Curie-Weiss behavior of pseudospins- $\frac{1}{2}$ (see Fig. 2(a-b)). Nevertheless, the excited CEF levels produce a sizeable Van Vleck term χ_{vv} .

To determine the χ_{vv} , we measured field-dependent magnetization at 0.45 K using a triply compensated extraction magnetometer within a 65 T short-pulse magnet at the National High Magnetic Field Laboratory, Los Alamos. As seen in Fig. 2(c), NaYbO_2 saturates around 16 T. The magnetization increases linearly in higher fields, and its slope corresponds to the van Vleck term of $\chi_{\text{vv}} = 0.0101 \mu_B/T = 0.00564 \text{ emu/mol/Oe}$ [33]. After subtracting this Van Vleck contribution, we arrive at the saturation magnetization of $1.75 \mu_B/\text{f.u.}$ Magnetic susceptibility with χ_{vv} subtracted follows the Curie-Weiss law with the effective moment of $\mu_{\text{eff}} = 2.84(2) \mu_B$. Both values are comparable favorably to $1.5 \mu_B/\text{f.u.}$ and $2.60 \mu_B$ expected from the powder-averaged $\bar{g} = 3.00$ calculated based on the CEF fit.

Low-temperature thermodynamics. The susceptibility fit also yields the Curie-Weiss temperature $\Theta = -5.64(1) \text{ K}$. Its negative value confirms antiferromagnetic interactions between the Yb^{3+} pseudospins. The absolute value is about two times larger than in YbMgGaO_4 ($\Theta_{\parallel} = -1.5 \text{ K}$, $\Theta_{\perp} = -2.7 \text{ K}$ [7]) and corroborates the two-fold increase in the sat-

uration field from 8 T in YbMgGaO₄ to 16 T in NaYbO₂. The simple estimate $\Theta = -3\bar{J}_1/2$ for a triangular antiferromagnet yields $\bar{J}_1 \simeq 3.8$ K, the energy scale of nearest-neighbor exchange couplings in NaYbO₂.

To probe low-temperature thermodynamics, we measured specific heat (C_p) of NaYbO₂ using the PPMS (Quantum Design) down to 0.4 K and a home-built dilution-fridge setup down to 70 mK [33]. Magnetic contribution to the C_p becomes visible below 8 K and shows a broad maximum around 1 K [33]. At even lower temperatures, magnetic contribution decreases without showing any signatures of a magnetic transition (see Fig. 2(d)). This suggests the absence of long-range magnetic order and the possibility of a spin-liquid state confirmed by the muon spin rotation (μ SR) measurement below.

By taking NaLuO₂ as the isostructural non-magnetic compound, we confirmed that lattice contribution to the C_p is negligible below 2 K, whereas the nuclear contribution was subtracted by systematic measurements in weak applied fields [33]. The remaining, magnetic contribution $C_m(T)$ will usually take the exponential form, $e^{-\Delta/T}$, or the form of a power law, T^p , for gapped and gapless excitations, respectively. However, neither term accounts for our experimental data (Fig. 2(d)). We tentatively fit $C_m(T)$ with two power laws, $aT^p + bT^q$, where $p \simeq 2.9$ resembles the T^3 contribution of magnons in a long-range-ordered antiferromagnet, and $q \simeq 0.5$ reflects a sublinear behavior, which is remotely similar to the power-law behavior in YbMgGaO₄ [6]. At first glance, a combination of the two different contributions could be seen as an effect of sample inhomogeneity, but a weak applied field restores the simpler $T^{2.2}$ power-law behavior [33], suggesting an intrinsic nature of the two power laws observed in zero field. We conclude that the low-energy excitations in NaYbO₂ are neither gapped nor magnon-like. They are also distinct from the low-energy excitations in YbMgGaO₄ that showed [6] the robust $T^{0.7}$ power law characteristic of the "spinon metal" of a U(1) quantum spin liquid [39].

Before going further, we note in passing that the magnetization curve of NaYbO₂ measured at 0.45 K shows a plateau between 4 and 5 T at about one half of the saturation magnetization as shown in Fig. 2(c). Such a $\frac{1}{2}$ -plateau contrasts with the $\frac{1}{3}$ -plateau typically observed in Heisenberg and XXZ triangular antiferromagnets [5] and may be indicative of a more complex interaction regime. Moreover, field-induced phase transitions should occur in NaYbO₂, but they go beyond the scope of our present manuscript and will be addressed in future studies.

μ SR data. Our heat-capacity data exclude long-range magnetic ordering above 70 mK, yet spin freezing would have no immediate effect on the specific heat. A direct probe of spin dynamics is thus essential to identify the QSL. To this end, we carried out zero-field (ZF) and longitudinal-field (LF) μ SR measurement down to 100 mK at the MuSR spectrometer (ISIS).

Four representative ZF μ SR spectra are shown in Fig. 3(a). They reveal neither oscillations nor a drastic drop in the initial asymmetry, indicative of the long-range magnetic order, but instead show signatures of persistent spin dynamics, in

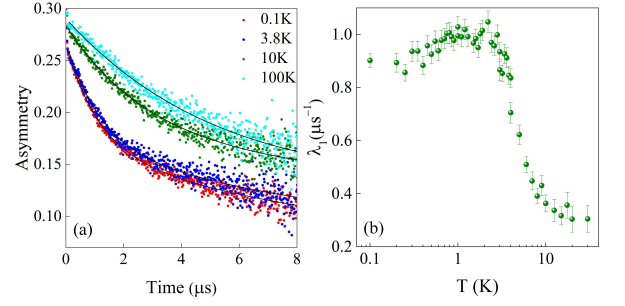


FIG. 3. (a) ZF μ SR spectra collected at various temperatures. The solid lines represent the fit using function (1). (b) Temperature dependence of the muon spin relaxation rate for the ZF μ SR spectra.

particular the lack of polarization recovery to $\frac{1}{3}$ of the initial value rules out the presence of static random fields. We further analyze these data by fitting the muon spectra with two exponential components:

$$A(t) = A_0[f_1 \exp(-\lambda_1 t) + (1 - f_1) \exp(-\lambda_2 t)] + B_0 \quad (1)$$

where A_0 and B_0 denote the initial asymmetry and the constant background, respectively, λ_1 and λ_2 represent the muon spin relaxation rates for muons implanted at two sites near O²⁻, f_1 stands for the fraction of the first component. The fitted ZF μ SR relaxation rate λ_1 , λ_2 and f_1 as a function of temperature are shown in [33]. f_1 shows temperature-independent behavior with its value close to 0.5, suggesting the same population at the two muon sites. Below we will discuss the electronic dynamics in terms of λ_1 since it is significantly larger than λ_2 .

Temperature dependence of λ_1 tracks the onset of correlations between the Yb³⁺ pseudospins. As seen in Fig. 3(b). Above 10 K, NaYbO₂ is paramagnetic with a smaller and temperature-independent λ_1 . The increase in λ_1 below 10 K is accompanied by the growing magnetic contribution to the specific heat, whereas the second temperature-independent regime below 2 K indicates the onset of the spin-liquid state. To prove the dynamic nature of the relaxation in this temperature range, we performed the LF experiment at 1.5 K. Should the relaxation arise from a weak static field, the size of this field is $B_{\text{loc}} = \lambda/\gamma_\mu \simeq 1.2$ mT, where $\gamma_\mu = 135.5 \times 2\pi \text{ s}^{-1} \mu\text{T}^{-1}$ is the gyromagnetic ratio for muons. Our LF data show that the relaxation persists in much higher fields, thus proving the dynamic nature of the Yb³⁺ pseudospins [33].

We also note that the characteristic evolution of λ_1 , its increase below 10 K and the saturation below 2 K, takes place at about twice higher temperatures compared to YbMgGaO₄ [8]. This further supports our conclusion on the twice stronger exchange couplings in NaYbO₂.

Low-energy excitations. The most interesting property of a spin liquid is arguably its excitation spectrum. We probed the low-energy excitations of NaYbO₂ at the cold-neutron multi-chopper LET spectrometer (ISIS) [40] at 45 mK using incident neutron energies of 1.46, 3.7, and 7.52 meV. Spectral weight observed above 0.8 \AA^{-1} is continuously distributed

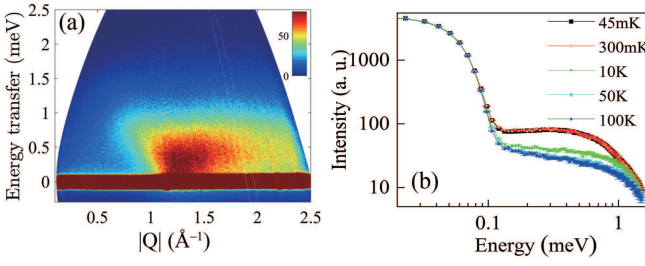


FIG. 4. (a) INS spectra measured at 45 mK with the incident energies $E_i=3.7$ meV. (b) Energy dependence of the integrated cut along Q in the range of $1.2\text{--}1.5 \text{ \AA}^{-1}$.

in both energy (E) and momentum (Q) and extends to about 1 meV (see Fig. 4(a)). This low-energy spectral weight concentrates around $Q \simeq 1.25 \text{ \AA}^{-1}$ corresponding to the K -point of the Brillouin zone with the reciprocal-lattice vector $(\frac{1}{3}, \frac{1}{3}, 0)$. A 120° magnetic order will lead to a Bragg peak at the same position, but the excitation spectrum is clearly different from the spin-wave spectrum of such an ordered state [33]. The energy dependence over the constant- Q cut suggests that the excitations reach low energies down to the elastic line that becomes prominent below 0.1 meV. This further confirms gapless nature of the magnetic excitations in NaYbO_2 (see Fig. 4(b)).

The spectrum of NaYbO_2 bears close similarities to that of YbMgGaO_4 , where no spectral weight was observed at low Q , around the zone center. All the spectral weight is concentrated in the vicinity of the zone boundary, in agreement with our observation of the spectral weight above 0.8 \AA^{-1} only. A further, and more subtle feature of YbMgGaO_4 , is the re-distribution of the spectral weight upon heating that signals the formation of distinct excitations at energies above and below \bar{J}_1 [11]. No such effect is seen in NaYbO_2 . Moreover, magnetic excitations in YbMgGaO_4 extend to the much higher energy of 2 meV, despite the fact that \bar{J}_1 is twice smaller than in NaYbO_2 .

Discussion. NaYbO_2 shows strong similarities to the widely studied triangular spin-liquid candidate YbMgGaO_4 except for the absence of structural disorder. Both materials entail the trigonally distorted YbO_6 octahedra. The CEF excitations of Yb^{3+} occur at about the same energies, and the compositions of the ground-state Kramers doublets are similar too. Exchange couplings differ by a factor of 2, though. This change is accompanied by a reduction in the Yb–O–Yb bridging angle from 99.4° in YbMgGaO_4 to 95.7° in NaYbO_2 .

The similarity between the two materials gives us an interesting opportunity to explore which of the effects reported for YbMgGaO_4 appear in the disorder-free case. Gapless ground state is retained in NaYbO_2 . On the other hand, neither the simple power-law behavior of the low-temperature specific heat [6], nor the energy separation of the spin excitations [11] have been observed. Moreover, the spin excitations of NaYbO_2 extend to much lower energies despite the twice larger \bar{J}_1 . This goes in line with the theory of Ref. 12 that explains both effects in terms of quenched disorder in a

valence-bond solid. These effects are probably not generic to the spin-liquid state of triangular antiferromagnets.

Rau and Gingras [41] computed anisotropic nearest-neighbor exchange couplings for several triangular geometries inspired by the possible local structures of YbMgGaO_4 . By extrapolating their results to the Yb–O–Yb angle of 95.7° in NaYbO_2 , we may expect that at least the nearest-neighbor coupling \bar{J}_1 in this material is very close to the Heisenberg limit. The second-neighbor interaction \bar{J}_2 should be then operative in order to stabilize a QSL. Such a scenario may be envisaged if, for example, \bar{J}_2 is less sensitive to the structural geometry than \bar{J}_1 . With $\bar{J}_2/\bar{J}_1 = 0.18(7)$ reported for YbMgGaO_4 [18], the increase in \bar{J}_1 accompanied by a small change in \bar{J}_2 will drive the system directly into the QSL phase [42]. Another interesting observation is that static structure factor calculated for this QSL phase peaks at the K -point of the Brillouin zone [28] in agreement with the accumulation of the low-energy spectral weight at $Q \simeq 1.25 \text{ \AA}^{-1}$ observed in our experiment (see Fig. 4), whereas YbMgGaO_4 shows a larger low-energy spectral weight at the M -point with the reciprocal-lattice vector $(\frac{1}{2}, 0, 0)$ [14]. All these arguments give a strong envision that the spin-liquid state observed in NaYbO_2 is the QSL phase of triangular antiferromagnets. Its gapless nature and unusual sensitivity to the magnetic field open prospects for future studies theoretically and experimentally.

Conclusions. The disorder-free NaYbO_2 gives the most direct experimental access to the spin-liquid physics of triangular antiferromagnets. Thermodynamic measurements and muon spectroscopy indicate the absence of magnetic order and persistent spin dynamics down to at least 70 mK. An excitation continuum is observed, with the spectral weight accumulating around the K -point, as expected in the QSL phase(s) driven by the exchange anisotropy or second-neighbor coupling on the triangular lattice [28]. The spin-liquid state of NaYbO_2 is gapless with a non-trivial low-temperature evolution of the specific heat, which does not follow the spinon scenario originally proposed for YbMgGaO_4 .

LD acknowledges support from the Rutherford International Fellowship Programme (RIFP). This project has received funding from the European Union's Horizon 2020 research and innovation programme under the Marie Skłodowska-Curie grant agreements No.665593 awarded to the Science and Technology Facilities Council. RDJ acknowledges financial support from the Royal Society. The work in Augsburg was supported by the German Science Foundation under TRR80. LD thanks G. Stenning for his help during the thermodynamic measurements in the Materials Characterisation Laboratory and P. Biswas during the muon data collection at the ISIS facility. AT thanks Yuesheng Li, Mayukh Majumder, Michael Baenitz, and Liviu Hozoi for useful discussions, and ESRF for providing the beamtime at ID22.

* lei.ding.ld@outlook.com; lei.ding@stfc.ac.uk

- [1] L. Balents, “Spin liquids in frustrated magnets,” *Nature* **464**, 199 (2010).
- [2] L. Savary and L. Balents, “Quantum spin liquids: a review,” *Rep. Prog. Phys.* **80**, 016502 (2017).
- [3] J. Knolle and R. Moessner, “A field guide to spin liquids,” *Annu. Rev. Condens. Matter Phys.* **10**, null (2019).
- [4] P. W. Anderson, “Resonating valence bonds: A new kind of insulator?” *Mater. Res. Bull.* **2**, 153 (1973).
- [5] O. Starykh, “Unusual ordered phases of highly frustrated magnets: a review,” *Rep. Prog. Phys.* **0830**, 22 (2015).
- [6] Y. S. Li, H. J. Liao, Z. Zhang, S. Y. Li, F. Jin, L. S. Ling, L. Zhang, Y. M. Zou, L. Pi, Z. R. Yang, J. F. Wang, Z. H. Wu, and Q. M. Zhang, “Gapless quantum spin liquid ground state in the two-dimensional spin-1/2 triangular antiferromagnet YbMgGaO₄,” *Sci. Rep.* **5**, 16419 (2015).
- [7] Y. Li, G. Chen, W. Tong, L. Pi, J. Liu, Z. Yang, X. Wang, and Q. Zhang, “Rare-earth triangular lattice spin liquid: A single-crystal study of YbMgGaO₄,” *Phys. Rev. Lett.* **115**, 167203 (2015).
- [8] Y. S. Li, D. Adroja, P. K. Biswas, P. J. Baker, Q. Zhang, J. Liu, A. A. Tsirlin, P. Gegenwart, and Q. M. Zhang, “Muon spin relaxation evidence for the U(1) quantum spin-liquid ground state in the triangular antiferromagnet YbMgGaO₄,” *Phys. Rev. Lett.* **117**, 097201 (2016).
- [9] Y. Shen, Y. D. Li, H. L. Wo, Y. S. Li, S. D. Shen, B. Y. Pan, Q. S. Wang, H. C. Walker, P. Steffens, M. Boehm, Y. Q. Hao, D. L. Quintero-Castro, L. W. Harriger, M. D. Frontzek, L. J. Hao, S. Q. Meng, Q. M. Zhang, G. Chen, and J. Zhao, “Evidence for a spinon Fermi surface in a triangular-lattice quantum-spin-liquid candidate,” *Nature* **540**, 559 (2016).
- [10] Y. Shen, Y. D. Li, H. L. Wo, Y. S. Li, S. D. Shen, B. Y. Pan, Q. S. Wang, H. C. Walker, P. Steffens, M. Boehm, Y. Q. Hao, D. L. Quintero-Castro, L. W. Harriger, M. D. Frontzek, L. J. Hao, S. Q. Meng, Q. M. Zhang, G. Chen, and J. Zhao, “Fractionalized excitations in the partially magnetized spin liquid candidate YbMgGaO₄,” *Nat. Commun.* **9**, 4138 (2018).
- [11] Y. S. Li, D. Adroja, D. Voneshen, R. I. Bewley, Q. M. Zhang, A. A. Tsirlin, and P. Gegenwart, “Nearest-neighbour resonating valence bonds in YbMgGaO₄,” *Nat. Commun.* **8**, 15814 (2017).
- [12] I. Kimchi, A. Nahum, and T. Senthil, “Valence bonds in random quantum magnets: theory and application to YbMgGaO₄,” *Phys. Rev. X* **8**, 031028 (2018).
- [13] Y. Xu, J. Zhang, Y. S. Li, Y. J. Yu, X. C. Hong, Q. M. Zhang, and S. Y. Li, “Absence of magnetic thermal conductivity in the quantum spin-liquid candidate YbMgGaO₄,” *Phys. Rev. Lett.* **117**, 267202 (2016).
- [14] J. A. M. Paddison, M. Daum, Z. L. Dun, G. Ehlers, Y. H. Liu, M. B. Stone, H. D. Zhou, and M. Mourigal, “Continuous excitations of the triangular-lattice quantum spin liquid YbMgGaO₄,” *Nat. Phys.* **13**, 117 (2017).
- [15] Y. S. Li, D. Adroja, R. I. Bewley, D. Voneshen, A. A. Tsirlin, P. Gegenwart, and Q. M. Zhang, “Crystalline electric-field randomness in the triangular lattice spin-liquid YbMgGaO₄,” *Phys. Rev. Lett.* **118**, 107202 (2017).
- [16] Z. Y. Zhu, P. A. Maksimov, S. R. White, and A. L. Chernyshev, “Disorder-induced mimicry of a spin liquid in YbMgGaO₄,” *Phys. Rev. Lett.* **119**, 157201 (2017).
- [17] E. Parker and L. Balents, “Finite-temperature behavior of a classical spin-orbit-coupled model for YbMgGaO₄ with and without bond disorder,” *Phys. Rev. B* **97**, 184413 (2018).
- [18] X. S. Zhang, F. Mahmood, M. Daum, Z. L. Dun, J. A. M. Paddison, N. J. Laurita, T. Hong, H. D. Zhou, N. P. Armitage, and M. Mourigal, “Hierarchy of exchange interactions in the triangular-lattice spin liquid YbMgGaO₄,” *Phys. Rev. X* **8**, 031001 (2018).
- [19] M. E. Zhitomirsky and A. L. Chernyshev, “Colloquium: Spontaneous magnon decays,” *Rev. Mod. Phys.* **85**, 219–243 (2013).
- [20] R. Kaneko, S. Morita, and M. Imada, “Gapless spin-liquid phase in an extended spin-1/2 triangular Heisenberg model,” *J. Phys. Soc. Jpn.* **83**, 093707 (2014).
- [21] W.-J. Hu, S.-S. Gong, W. Zhu, and D. N. Sheng, “Competing spin-liquid states in the spin- $\frac{1}{2}$ Heisenberg model on the triangular lattice,” *Phys. Rev. B* **92**, 140403(R) (2015).
- [22] Z. Zhu and S. R. White, “Spin liquid phase of the $S = 1/2$ $J_1 - J_2$ Heisenberg model on the triangular lattice,” *Phys. Rev. B* **92**, 041105(R) (2015).
- [23] R. F. Bishop and P. H. Y. Li, “Spin-gap study of the spin- $\frac{1}{2}$ $J_1 - J_2$ model on the triangular lattice,” *Europhys. Lett.* **112**, 67002 (2015).
- [24] Y. Iqbal, W.-J. Hu, R. Thomale, D. Poilblanc, and F. Becca, “Spin liquid nature in the Heisenberg $J_1 - J_2$ triangular antiferromagnet,” *Phys. Rev. B* **93**, 144411 (2016).
- [25] S. N. Saadatmand and I. P. McCulloch, “Symmetry fractionalization in the topological phase of the spin- $\frac{1}{2}$ $J_1 - J_2$ triangular Heisenberg model,” *Phys. Rev. B* **94**, 121111(R) (2016).
- [26] D.-V. Bauer and J. O. Fjærestad, “Schwinger-boson mean-field study of the $J_1 - J_2$ Heisenberg quantum antiferromagnet on the triangular lattice,” *Phys. Rev. B* **96**, 165141 (2017).
- [27] S.N. Saadatmand and I.P. McCulloch, “Detection and characterization of symmetry-broken long-range orders in the spin- $\frac{1}{2}$ triangular Heisenberg model,” *Phys. Rev. B* **96**, 075117 (2017).
- [28] Z. Y. Zhu, P. A. Maksimov, Steven R. White, and A. L. Chernyshev, “Topography of spin liquids on a triangular lattice,” *Phys. Rev. Lett.* **120**, 207203 (2018).
- [29] P.A. Maksimov, Z. Zhu, S.R. White, and A.L. Chernyshev, “Anisotropic-exchange magnets on a triangular lattice: spin waves, accidental degeneracies, and dual spin liquids,” arXiv:1811.05983.
- [30] M. Baenitz, Ph. Schlender, J. Sichelschmidt, Y. A. Onyikienko, Z. Zangeneh, K. M. Ranjith, R. Sarkar, L. Hozoi, H. C. Walker, J.-C. Orain, H. Yasuoka, J. van den Brink, H. H. Klauss, D. S. Inosov, and Th. Doert, “NaYbS₂: A planar spin-1/2 triangular-lattice magnet and putative spin liquid,” *Phys. Rev. B* **98**, 220409 (2018).
- [31] W. W. Liu, Z. Zhang, J. T. Ji, Y. X. Liu, J. S. Li, and H. C. Lei, “Rare-earth chalcogenides: A large family of triangular lattice spin liquid candidates,” *Chin. Phys. Lett.* **35**, 1 (2018).
- [32] Y. Hashimoto, M. Wakeshima, and Y. Hinatsu, “Magnetic properties of ternary sodium oxides NaLnO₂ (Ln = rare earths),” *J. Solid State Chem.* **176**, 266 (2003).
- [33] See Supplemental Material for an additional description of the experimental methods, crystal structure refinements, details of the CEF fit, and analysis of the low-temperature heat capacity.
- [34] L. C. Chapon *et al.*, “Wish: The new powder and single crystal magnetic diffractometer on the second target station,” *Neutron News* **22**, 22–25 (2011).
- [35] J. Gaudet, D. D. Maharaj, G. Sala, E. Kermarrec, K. A. Ross, H. A. Dabkowska, A. I. Kolesnikov, G. E. Granroth, and B. D. Gaulin, “Neutron spectroscopic study of crystalline electric field excitations in stoichiometric and lightly stuffed Yb₂Ti₂O₇,” *Phys. Rev. B* **92**, 134420 (2015).
- [36] K. A. Ross, L. Savary, B. D. Gaulin, and L. Balents, “Quantum excitations in quantum spin ice,” *Phys. Rev. X* **1**, 021002 (2011).
- [37] R. I. Bewley, R. S. Eccleston, K. A. McEwen, S. M. Hayden, M. T. Dove, S. M. Bennington, J. R. Treadgold, and R. L. S. Coleman, “MERLIN, a new high count rate spectrometer at ISIS,” *Phys. B: Condens. Matter* **385-386**, 1029 (2006).
- [38] Y.-D. Li, X. Wang, and G. Chen, “Anisotropic spin

- model of strong spin-orbit-coupled triangular antiferromagnets,” *Phys. Rev. B* **94**, 035107 (2016).
- [39] O. I. Motrunich, “Variational study of triangular lattice spin-12 model with ring exchanges and spin liquid state in κ -(ET)₂Cu₂(CN)₃,” *Phys. Rev. B* **72**, 045105 (2005).
- [40] R. I. Bewley, J. W. Taylor, and S. M. Bennington, “LET, a cold neutron multi-disk chopper spectrometer at ISIS,” *Nucl. Instr. Meth. Phys. Res. Sect. A* **637**, 128 (2011).
- [41] J.G. Rau and M.J.P. Gingras, “Frustration and anisotropic exchange in ytterbium magnets with edge-shared octahedra,” *Phys. Rev. B* **98**, 054408 (2018).
- [42] One could argue that \bar{J}_2 increases as well, but $\bar{J}_1 \simeq 3.8$ K will then lead to \bar{J}_2 of nearly 1 K, which is hard to reconcile with the second-neighbor Yb–Yb distance of 5.82 Å and the strongly localized nature of f -electrons in Yb³⁺.